Sensing and Bio-Sensing Research 50 (2025) 100927

Contents lists available at ScienceDirect

Sensing and Bio-Sensing Research

journal homepage: www.elsevier.com/locate/sbsr

Electrochemical detection of choline *via* oxygen consumption in a thermally reduced graphene oxide matrix: Advantages of operation at both positive and negative potentials

Ieva Sakinyte-Urbikiene [a,*], Marius Butkevicius [a], Vidute Gureviciene [a], Liubov Galuzinska [b], Julija Razumiene [a]

[a] Department of Bioanalysis, Institute of Biochemistry, Life Sciences Center, Vilnius University, Sauletekio av. 7, Vilnius LT- 10257, Lithuania
[b] National University of Pharmacy, Ministry of Health of Ukraine, Hryhoriia Skovorody str., 53, Kharkiv 61002, Ukraine

ARTICLE INFO

Keywords:
Amperometric biosensor
Choline oxidase
TRGO
Mechanism of choline bioelectrocatalysis
ORR

ABSTRACT

An amperometric choline biosensor was developed using synthesised thermally reduced graphene oxide (TRGO) as an efficient electrochemical surface and immobilisation matrix for choline oxidase (ChOx). The biosensor can operate *via* two distinct mechanisms depending on the applied working electrode potential: dissolved oxygen (O_2) consumption at −0.3 V and hydrogen peroxide oxidation at +0.6 V *vs* Ag/AgCl. Under these conditions, the TRGO/ChOx biosensor exhibited a linear response to choline concentrations of 0.0009–0.24 mM and 0.0008–0.24 mM, with sensitivities of 29 and 38 μA mM^{-1} cm^{-2} at −0.3 V and + 0.6 V *vs* Ag/AgCl, respectively. Operation at −0.3 V significantly improved biosensor selectivity by minimizing interference from common biological species, including dopamine, adenosine, serotonin, uric acid, ascorbic acid, glucose, albumin, and epinephrine. The TRGO/ChOx biosensor demonstrated excellent accuracy in mouse urine samples, yielding recovery rates of 101–107 % and relative standard deviations of 0.4–3.9 %. These features, including the dual operating mechanisms, highlight the strong potential of this biosensor for rapid and reliable choline detection in non-invasive diagnostics.

1. Introduction

Choline biosensors have garnered increasing attention due to their broad applicability in healthcare, neuroscience, and environmental monitoring. Their ability to selectively detect and quantify choline, a pivotal precursor to the neurotransmitter acetylcholine, renders them indispensable tools for investigating brain function and diagnosing neurological disorders. In the context of neurological research and clinical diagnostics, choline biosensors play a crucial role in elucidating brain chemistry, as choline is closely linked to cognitive performance and memory. Dysregulation of choline metabolism has been implicated in the pathogenesis of neurodegenerative diseases such as Alzheimer's and Parkinson's disease [1–3]. Biosensor enhancement innovations are continually appreciated, as they facilitate real-time monitoring of choline concentrations, providing valuable insights into neurotransmitter dynamics and enabling the early detection of neurological dysfunctions [2]. Choline biosensors contribute significantly to the advancement of personalised medicine by supporting continuous monitoring of dietary intake and metabolic variations. This information can individualise nutritional strategies and therapeutic decisions, particularly for managing metabolic syndromes and related health conditions [4–6]. Moreover, by combining choline biosensors with choline esterases or their specific substrates and inhibitors, it is possible to create analytical systems capable of determining not only choline but also acetylcholine and cholinesterase activities in various biological samples (brain tissue homogenates, dialysate samples, human serum), thereby improving the prognosis and diagnosis of multiple diseases using only a single biosensor [7–11]. Accordingly, it is critical that the choline biosensor under development exhibits high selectivity and sensitivity, and functions through a clearly defined mechanism that remains unaffected by any interfering compounds.

Over the last few decades, various choline oxidase (ChOx)-based biosensors for detecting choline have been designed, utilizing optical (*e.g.*, colorimetry, fluorescence, electrochemiluminescence),

* Corresponding author.
E-mail addresses: ieva.sakinyte@gmc.vu.lt (I. Sakinyte-Urbikiene), marius.butkevicius@gmc.vu.lt (M. Butkevicius), vidute.gureviciene@gmc.vu.lt (V. Gureviciene), julija.razumiene@gmc.vu.lt (J. Razumiene).

https://doi.org/10.1016/j.sbsr.2025.100927
Received 15 October 2025; Received in revised form 21 November 2025; Accepted 24 November 2025
Available online 26 November 2025

chemiluminescence, or electrochemical approaches [3]. Electrochemical biosensors, as a potent analytical tool, are emerging to hold a distinct niche for quick screening of choline. Amperometric choline biosensors are particularly important among them because of their many benefits, including low cost, ease of design, and real-time monitoring of choline levels even in turbid media. The selectivity of proposed biosensors is ensured by the enzyme ChOx. ChOx selectively converts choline to betaine and H_2O_2, enabling precise detection [12–14]. The enhanced electrochemical performance of designed sensors is achieved mainly through the modifications of bare electrode surfaces because this solves key challenges such as ensuring efficient electron transport and stabilizing the enzyme activity itself by immobilizing it into the electrode surface matrix. Actually, it explains why many of them have intricate designs that frequently include multiple layers of supporting materials and additional mediators [3,15–18].

Although numerous amperometric choline biosensors based on ChOx have been developed, they face challenges in interference, long-term stability, narrow linear range, and, in many cases, the underlying sensing mechanisms remain poorly understood or are merely attributed to the electrochemical decomposition of hydrogen peroxide at the electrode surface [3]. These restrictions continue to be addressed by breakthroughs in nanomaterials research and membrane design [12,19–23].

The aforementioned obstacles were overcome in this study by designing biosensors using immobilized ChOx in a thermally reduced graphene oxide (TRGO) matrix. Furthermore, understanding how sensing mechanisms depend on the applied electrode working potential helped develop a choline biosensor that operates through a dual mechanism.

In fact, graphene-based nanomaterials possess several advantageous characteristics, notably the presence of electroactive oxygen-containing functional groups, such as quinones, that can actively participate in electron transfer (ET) with redox-active enzymes [23,24]. These oxygen functional groups enable TRGO to directly transfer or receive electrons from enzymes, or to electrochemically activate enzymatic reaction products, thus eliminating the need for additional redox mediators. The absence of mediators represents a major advantage for biosensor design, as it enhances selectivity by allowing operation at potentials closer to the intrinsic redox potential of the enzyme, thereby minimizing interference and simplifying the reaction mechanism [23,25]. Moreover, graphene-based nanomaterials exhibit excellent electrical conductivity, a high specific surface area, active sites in structural defects, and superior biocompatibility compared to many other conventional materials [26,27]. Due to these properties, TRGO may also participate in the oxygen reduction reaction (ORR). It is known that oxygen-containing functional groups introduce structural defects and vacancies, serve as active sites for O_2 adsorption and dissociation. Adjacent carbon atoms near oxygen become electron-deficient and promoting O_2 adsorption and electron transfer. Moreover, localized positive charges stabilize oxygen reduction intermediates. Thus, oxygen containing functional groups lower the energy barrier for O—O bond cleavage, favouring the 4-electron pathway (direct reduction to H_2O) over the less efficient 2-electron pathway [28–30].

Several works have been found in the literature describing that ORR occurs in biosensors based on graphene derivatives and oxidase enzymes, which catalyse substrate-specific reactions leading to the depletion of dissolved O_2 at negative potentials [31–33]. However, a thorough description of the ChOx catalytic mechanism, as reported in this paper, for the biosensor operating at negative potentials, has been proposed for the first time. Understanding the mechanism enables increased process efficacy, which is crucial since electrochemical biosensors that utilize local O_2 consumption are a promising tool for various biochemical analyses. These sensors often rely on enzymatic reactions that consume O_2, allowing for the detection of specific analytes through changes in dissolved O_2 concentration. The occurrence of the ORR on the surface of TRGO allows to create construction of a biosensor capable of operating at negative potentials. One of the key advantages of this condition is reduced interference: electroactive species that typically interfere at positive potentials remain inactive at negative potentials, thereby minimizing noise and improving signal accuracy. Moreover, ORR at negative potentials avoids false signals caused by other oxidizable molecules [34].

The suggested electrode material also shows significant potential for advancing sustainable energy technologies where O_2 reduction is a basic electrochemical process. Due to ORR is often the rate-limiting step possessing slow kinetics and high overpotentials, the used electrode material becomes crucial. While Pt remains the benchmark, future progress depends on cost-effective, durable, and scalable alternatives. Next-generation ORR catalysts that can power a sustainable energy future.

In our work was developed biosensor using TRGO and ChOx choline oxidase from *Arthrobacter globiformis* (EC 1.1.3.17) operating on dissolved O_2 consumption mechanism at negative working electrode potential. After examining the main mechanistic aspects of the biosensor, it became apparent that it could operate according to two mechanisms as needed simply by changing the potential of the working electrode. Due to this, it has a high potential for the rapid and reliable non-invasive detection of choline in urine samples.

2. Materials and methods

2.1. Materials

Choline oxidase (EC 1.1.3.17, 17 U/mg) from *Arthrobacter globiformis* and glucose oxidase from (EC 1.1.3.4, 228253 U/g) *Aspergillus niger* purchased from Sigma. Second fraction of thermaly reduced graphene oxide (TRGO) was synthesised according to [23]. Hydrogen peroxide, (30 %, *v*/v aqueous solution), choline chloride, betaine aldehyde chloride (BA), glycine betaine (GB), adenosine 5′-diphophate, serotonin hydrochloride, uric acid, ascorbic acid, D-glucose, bovine serum albumin (V fraction) (BSA), dopamine hydrochloride, epinephrine, polyvinylalcohol (PVA), polyethylenimine were obtained from Sigma. Glutaraldehyde 25 % was obtained from Merck KGaA. Semipermeable polyester (PETE) membrane filters, 12 μM thickness, 0.4 μM diameter of pore were obtained from Sterlitech, USA. The urine samples from mouse were obtained from National University of Pharmacy, Ukraine.

A 0.02 M phosphate buffer solution (PBS) was prepared by mixing stock solutions of KH_2PO_4 and Na_2HPO_4. All other chemicals were of analytical grade and used without further purification. All aqueous solutions were prepared with distilled water.

2.2. Preparation of biosensor and electrochemical measurements

Firstly, a round of semipermeable PETE film was fixed to a rubber ring with an inner diameter of 3 mm. To prepare the enzymatic membranes, a 50 μL mixture containing 0.5 mg of ChOx, 2 mg of TRGO, 1 mg of bovine serum albumin (BSA) and 2 μL of 5 % glutaraldehyde was prepared in PBS. Subsequently, 5 μL of this mixture was deposited onto the inner surface of the membrane fixed within the ring and allowed to set at 4 °C overnight. In this case, TRGO serves the dual function of both enzyme immobilisation matrix and electrode material. The prepared enzymatic membrane was pressed onto the surface of a graphite rod electrode by forming biosensor (TRGO/ChOx). To evaluate the effect of TRGO on ChOx and the O_2 reduction reaction (ORR), a control sensor was fabricated in the same manner, without incorporating ChOx into the enzymatic membrane. In this case, the membrane lacking ChOx was attached to a graphite electrode, forming the control biosensor (TRGO). To further demonstrate the significance of TRGO properties for the biosensor's performance, an additional enzymatic membrane without TRGO was prepared and attached to a platinum (Pt) electrode surface, which is well known as an excellent electrode material for biosensors employing oxidases as biorecognition elements [35].

Chronoamperometric measurements were conducted using a custom-made potentiostat (Vilnius University, Life Sciences Centre, Institute of Biochemistry), which utilized a conventional three-electrode electrochemical cell comprising a platinum auxiliary electrode, a saturated Ag/AgCl reference electrode, and the biosensor as the working electrode. These measurements were conducted in a 1 mL thermostated electrochemical cell at 20 °C. The current-time responses of the biosensor to multiple concentrations of choline, H_2O_2, betaine aldehyde, glycine betaine, adenosine, serotonin, uric acid, ascorbic acid, D-glucose, bovine serum albumin, dopamine, and epinephrine in PBS were monitored at working potentials from −0.5 to +0.6 V *vs* Ag/AgCl in a stirred PBS buffer solution (pH 7.2). The performance of the biosensor was evaluated by comparing the current-time responses in relation to substrate concentration (C). The limit of detection (LOD) of the constructed biosensors was calculated from the linear part of the calibration curve according to [36]. The biosensor-generated signals were measured three times at the same choline concentration (0.05 mM) within the linear range of the calibration curve. The standard deviation of these signals was calculated, multiplied by 3, and divided by the slope of the linear part of the calibration curve, representing the sensitivity of the biosensor.

The long-term stability of the TRGO/ChOx biosensor was evaluated through consecutive measurements of the current response to a 0.3 mM choline solution. The stability of the TRGO/ChOx biosensors was assessed on their operational efficiency. Each day, the average response from twenty measurements was recorded over a one-month period. Between experiments, the biosensor was stored in PBS solution at room temperature.

The analytical recovery of the TRGO/ChOx biosensor was evaluated using the multiple-spike standard addition method. For this purpose, four different aliquots of tenfold-diluted mouse urine were spiked with 0.5 mM, 1.0 mM, 1.5 mM, and 2.5 mM concentrations of choline. The current–time responses of the TRGO/ChOx biosensor to 50 μL of each aliquot were recorded three times. The measured responses were converted to concentrations of choline using the calibration curve. The recovery for each added choline concentration was calculated according to Eq. (1).

$$\text{Recovery } (\%) = \left(C_{choline\ found} - C_{choline\ in\ urine}\right) / C_{choline\ added} \text{ x } 100\% \quad (1)$$

All the measurements were repeated at least three times, and the graphs present the mean values of the results.

3. Results

3.1. Study of TRGO/ChOx action mechanisms

The applied potential of a biosensor plays a pivotal role in determining the electrode signal and the overall sensor performance, as it governs which redox reactions can occur at the electrode surface. Undoubtedly, the nature of the electrode material also influences this dependency. Thus, at first, the effect of the applied potential on the biosensor response to choline and H_2O_2 was investigated, and the activity of the TRGO/ChOx is shown in Fig. 1.

The electrocatalytic conversions of 0.47 mM choline and 0.25 mM H_2O_2 were evaluated across a range from +0.6 to −0.5 V (Fig. 1). The responses of the TRGO/ChOx to choline are anodic across the entire potential measurement range. As the applied potential decreased from +0.6 to 0.2 V, the response current of the biosensor to choline correspondingly decreased. Between +0.2 and 0 V, the responses stabilized. Upon further shifting the potential from 0 to −0.4 V, the response current of the TRGO/ChOx exhibited an increase and reached a steady state beyond −0.4 V. Meanwhile, H_2O_2 oxidation occurs within the potential range of +0.6 V to 0 V. When the potential shifts more negatively, H_2O_2 reduction takes place (Fig. 1). These results suggest that the operating mechanism of the TRGO/ChOx is independent of the electrochemical

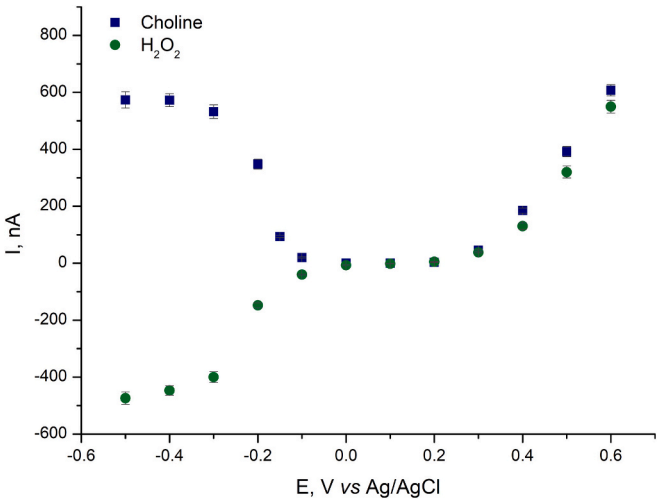

Fig. 1. Effect of applied electrode potential on the response of the TRGO/ChOx to 0.47 mM choline and 0.25 mM H_2O_2.

reduction of H_2O_2 at negative electrode potentials, whereas at positive electrode potentials, the biosensor operates primarily through the electrochemical oxidation of H_2O_2.

The available literature indicates that choline oxidase (E.C. 1.1.3.17) catalyses the two-step and four-electron oxidation reaction of choline to glycine betaine (GB). During the initial oxidation step, choline is converted to betaine aldehyde (BA), accompanied by the reduction of molecular O_2 to H_2O_2. In the second oxidation step, the enzyme-associated BA is hydrated, resulting in the formation of gem-diol-choline. This compound is then oxidised to GB, accompanied by the reduction of the second O_2 to H_2O_2 [37]. The overall reaction catalysed by ChOx is presented in Eq. (2).

$$2\ O_2 + \text{choline} \xrightarrow{ChOx} \text{Glycine betaine} + 2\ H_2O_2 \quad (2)$$

$$H_2O_2 \rightarrow H_2O + ½\ O_2 \quad (3)$$

$$O_2 + 2\ H^+ + 2\ e^- \rightarrow H_2O_2 \quad (4)$$

$$O_2 + 4\ H^+ + 4\ e^- \rightarrow 2\ H_2O \quad (5)$$

$$H_2O_2 + 2\ H^+ + 2\ e^- \rightarrow 2H_2O \quad (6)$$

This knowledge of the catalysing mechanism led to a series of experiments being conducted with the objective of investigating the possibility of oxidation and reduction of the choline oxidase products on the TRGO/ChOx electroactive surface at negative potentials. Fig. 2 presents typical anodic and cathodic current-time responses of the TRGO/ChOx and the control TRGO sensor to ChOx products at a potential of −0.3 V.

The addition of choline and BA to the electrochemical cell (at 30 s) generates an anodic signal of the biosensor, whereas GB has no influence on the signal. The TRGO/ChOx response to choline is approximately twice as high as that observed for BA. This can be attributed to the enzymatic pathway, wherein the oxidation of choline to GB by ChOx requires the consumption of two O_2 molecules and the production of two equivalents of H_2O_2, *via* a four-electron reduction pathway overall. While the catalysis of BA to GB involves only one O_2 *via* a two-electron reduction pathway [37]. The data presented in Fig. 2 shows that there is no direct oxidation of BA. Because in the case of direct oxidation of BA and using the same concentration of choline and BA, the change in current should be similar. The obtained current change ratio of 2:1 (Choline and BA) indicates that a change in O_2 content is most likely the cause of the current change.

Using the control sensor without ChOx, the introduction of choline, BA, and GB into the electrochemical system had no effect on the sensor

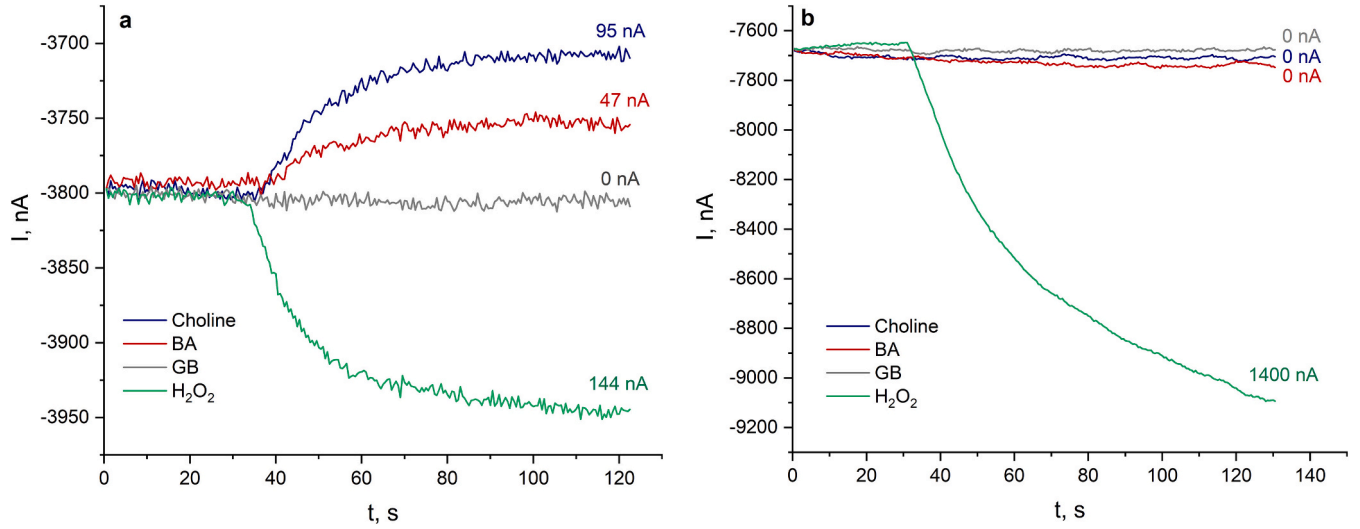

Fig. 2. Current-time responses of the TRGO/ChOx (a) and control TRGO sensor (b) to choline oxidase products: 0.05 mM choline, 0.05 mM betaine aldehyde (BA), 0.05 mM glycine betaine (GB), and 0.05 mM hydrogen peroxide. E = −0.3 V *vs* Ag/AgCl and PBS (0.01 M; pH 7.2).

signal; only the reduction of hydrogen peroxide was observed (Fig. 2 b). These findings support the hypothesis that the selective response of the TRGO/ChOx is characterised by the consumption of dissolved O_2 levels in the system as a result of ChOx's selective catalysis.

The negative background current of TRGO/ChOx at −0.3 V indicates that ORR can take place on TRGO surface as described in Eq. (4) and Eq. (5): the ORR proceeds *via* a $4e^-$ pathway, which reduces O_2 to H_2O (Eq. (5)), and the 2e- pathway (Eq. (4)), yielding H_2O_2. When the amount of O_2 in the system is reduced by the consumption in any enzymatic reaction, the anodic current-time response of the biosensor is observed as a result of the decrease of O_2 in ORR. Based on literature data, both processes occur simultaneously. This ORR pathway has been linked to the presence of oxygen functional groups on the surface of graphene derivatives [38,39]. Furthermore, data in the literature suggest that ORR occurs in biosensors based on graphene derivatives and oxidase enzymes catalysing substrate-specific reactions leading to the depletion of dissolved O_2 at negative potentials. Graphene-based materials, owing to their high surface area, abundant edge-plane active sites, and functional groups including heteroatoms effectively facilitate ORR and enhance the overall electrocatalytic performance of such biosensors [31–33]. Thus, TRGO possesses advantageous properties such as Brunauer–Emmett–Teller (BET) surface area of 689.5 ± 11.3 $m^2\ g^{-1}$ and an oxygen content of 9.7 W% in the form of organic functional groups [23]. It is evident that, owing to the properties of TRGO, the ORR can be facilitated within the system.

In order to verify that the change in current after the addition of choline is due to the consumption of oxygen during the reaction, an additional experiment was performed when D-glucose was added to the solution (30 s), followed by the addition of glucose oxidase (80 s) (Fig. 3).The biosensor's anodic current-time response reflects the decrease of amount of O_2 in ORR due to the consumption of O_2 in bioelectrocatalysis by GOx.

Dissolved O_2 is consumed by GOx during the 2e- reduction of O_2 to H_2O_2, while simultaneously oxidizing D-(+)-glucose to D-(+)-gluconoδ-lactone [33]. Fig. 3 shows that the addition of GOx causes a similar decrease in background current. Worth mentioning that H_2O_2 (produced by the oxidase enzyme reaction) reduces as well, so the biosensor's current-time response changes are due to the sum of these reduction events. The decrease in O_2 reduction is a more efficient process that determines the overall operation of the biosensor. This hypothesis was supported by experiments with a control sensor: TRGO without enzyme. A similar change in current was observed when D-glucose and GOx were added to the reaction mixture.

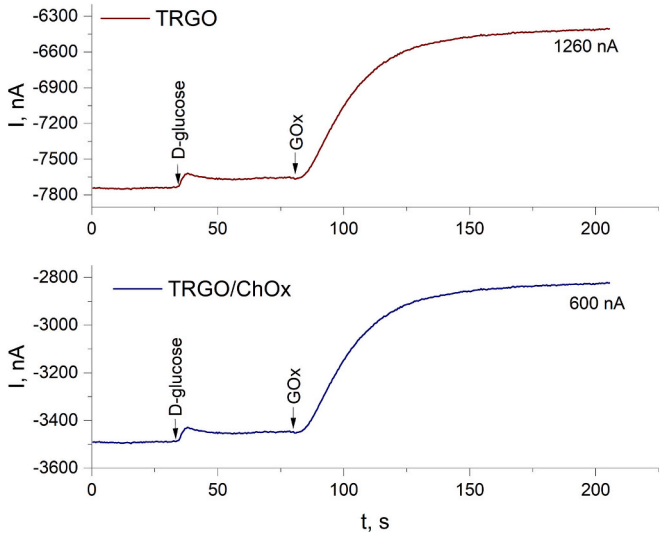

Fig. 3. Current-time responses of the TRGO/ChOx and TRGO sensor to 0.2 mM D-glucose and glucose oxidase (GOx). E = −0.3 V *vs* Ag/AgCl and PBS (0.01 M; pH 7.2).

As evidenced by the measurements obtained using sensor contained only TRGO, both the negative background current and the responses to hydrogen peroxide (tenfold increase) and glucose with GOx (twofold increase) were significantly higher compared to those observed with the TRGO/ChOx (Fig. 1 and Fig. 3). This is attributed to the absence of enzyme in the control membrane, what allows for a larger accessible TRGO surface area as well as, a greater number of active sites for oxygen molecules. Thus, it leads to more efficient ORR and hydrogen peroxide reduction. The assessments using the TRGO sensor were made with the specific purpose of evaluating the direct contribution of TRGO as electrode material to ORR and hydrogen peroxide reduction, in the absence of the influence of immobilized enzymes. Proposed detection mechanism offers several advantages, including a direct correlation with choline oxidase activity and substrate concentration, operation at lower applied potentials, minimal interference from electroactive species, and versatility as a universal platform applicable to many oxidase enzymes. However, it also has some limitations related to variations in dissolved oxygen concentration in the samples, which can be minimized through

proper management of oxygen supply.

The results obtained from this finding lend further credence to the hypothesis that the operation of the TRGO/ChOx biosensor is contingent upon the efficient consumption of dissolved O_2 by the TRGO at a negative working electrode potential. Overall, it confirms that the TRGO/ChOx biosensor can operate in two modes: through O_2 consumption within the negative electrode potential range and H_2O_2 oxidation within the positive electrode potential range.

3.2. Characterisation of TRGO/ChOx

After demonstrating the operation of the TRGO/ChOx, the task was to compare the benefits of biosensor performance by analysing real samples when the biosensor functions at both negative and positive potentials. Aiming to apply it for choline determination in mouse urine samples, the subsequent study was focused on evaluating the main biosensor characteristics, including sensitivity, stability, linear ranges, LOD and selectivity. At first, the dependences of the current density on choline concentration (calibration curves) at different working electrode potentials of −0.3 and + 0.6 V were obtained (Fig. 4). All summarized analytical parameters of the biosensors are presented in Table 1. The sensitivities of the biosensors were obtained from the slope of linear ranges. To demonstrate the significance of TRGO properties for the biosensor's performance, an additional enzymatic membrane without TRGO was prepared in the same manner and attached to a platinum electrode surface (Pt/ChOx), which is well known as an excellent electrode material for biosensors employing oxidases as biorecognition elements [35].

At the applied working electrode potential of +0.6 V, then hydrogen peroxide oxidation take place, both TRGO/ChOx and Pt/ChOx biosensors showed a linear response to choline in the range 0.0008–0.24 mM and 0.006–0.24 mM, with sensitivities of 38 and 6 μA mM^{-1} cm^{-2}, respectively. Compared to the Pt/ChOx biosensor, the TRGO/ChOx biosensor shows more than 5 times higher sensitivity. This increased sensitivity could be attributed to the large surface area of TRGO and its oxygen-containing functional groups, which are involved in electron transfer reactions between the active site of the enzyme and the graphite electrode surface [23]. At negative potential (−0.3 V) then TRGO/ChOx operates through dissolved O_2 consumption, a linear response to choline in the range 0.0009–0.24 mM, with sensitivity of 29 μA mM^{-1} cm^{-2} were observed. A comparison of the electroanalytical parameters of the proposed biosensors with previously reported choline biosensors [3,40,41] shows that their sensitivity and LOD are within the same order of magnitude or slightly lower. However, biosensors described in the literature differ substantially in their design, fabrication strategies, and the amount of immobilized ChOx—factors that can significantly influence sensitivity [40]. In this work, no additional electrochemical mediator was used, and the amount of enzyme (10 mg/mL stock solution) was optimized to achieve an appropriate balance between biosensor performance, cost, and practical applicability. The proposed biosensors exhibit a broad linear range, indicating their suitability for choline detection across a wide spectrum of biological samples.

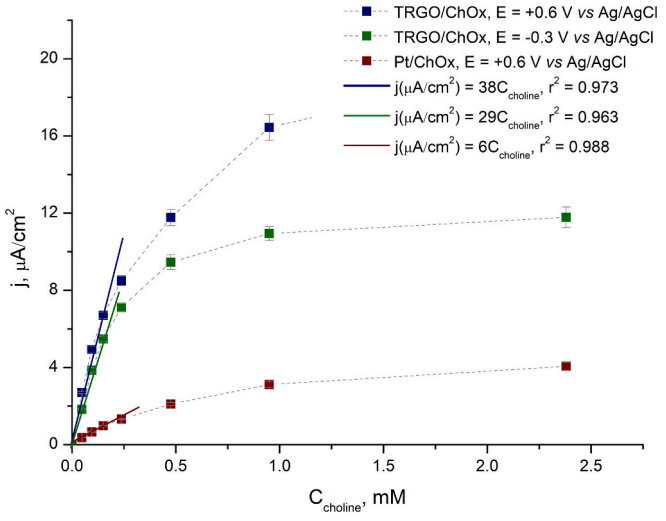

Fig. 4. Calibration curves and the linear ranges of the TRGO/ChOx and Pt/ChOx biosensors. E = +0.6 V and − 0.3 *vs* Ag/AgCl and PBS (0.01 M; pH 7.2).

Table 1
Comparison of electroanalytical parameters of the proposed biosensor.

Name	Sensitivity, μA mM^{-1} cm^{-2}	r^2	Linear range, mM	Working potential, V *vs* Ag/AgCl	LOD, μM
TRGO/ ChOx	29	0.963	0.0009–0.24	−0.3	0.9
TRGO/ ChOx	38	0.973	0.0008–0.24	+0.6	0.8
Pt/ChOx	6	0.988	0.006–0.24	+0.6	6.2

It is noteworthy that after 31 days of operation, the TRGO/ChOx biosensor retained 39 % of its initial sensitivity. This level of operational stability is comparable to the storage stability reported for other previously developed biosensors [3]. The relatively high stability observed may result from π–π interactions between the ChOx and the TRGO matrix, which help preserve the enzyme's structure and promote efficient electron transfer. Nevertheless, the gradual decrease in sensitivity can be attributed to ChOx inactivation and the degradation of oxygen-containing functional groups on the TRGO surface in the aqueous environment. These changes collectively led to a reduction in ORR capacity and a concomitant decrease in biosensor sensitivity.

The selectivity of the proposed TRGO/ChOx choline biosensor was evaluated at two applied electrode potentials as well by introducing dopamine (0.5 μM), adenosine (0.5 μM), serotonin (0.5 μM), uric acid (1 μM), ascorbic acid (2.5 μM), D-glucose (0.05 mM), albumin (70 g/l), epinephrine (24 μM) and choline (0.24 mM) into the electrochemical cell (Fig. 5 a and b).

As shown in Fig. 5 a, while biosensor TRGO/ChOx acting at +0.6 V, slight current increase was observed after the addition of potential interfering compounds such as dopamine, adenosine, serotonin, uric acid, D-glucose, albumin, and ascorbic acid (up to 5 %) compared with the response to epinephrine and choline. Meanwhile, at a working potential of −0.3 V, there is no current increase after adding potential interfering compounds, as well as epinephrine (Fig. 5 b). Thus, at negative potential the TRGO/ChOx biosensor exhibits characteristics comparable to those obtained at +0.6 V. As a compromise between achieving a sufficiently high analytical response and minimizing the influence of potential interferents, a working potential of −0.3 V was selected for further studies.

To make the biosensor suitable for non-invasive bioanalysis, its performance was evaluated using mouse urine samples. The selection of samples was determined by the fact that the developed biosensor will subsequently be used to assess changes in cholinesterase activity as novel non-invasive biomarkers for monitoring the dynamics of inflammatory processes and the effectiveness of pharmacological agents in model animal systems. The analytical recovery of the TRGO/ChOx biosensor, at a working potential of −0.3 V, was evaluated using the multiple-spike standard addition method. For this purpose, four different aliquots of tenfold-diluted mouse urine were spiked with 0.5 mM, 1.0 mM, 1.5 mM, and 2.5 mM concentrations of choline. The current–time responses of the TRGO/ChOx biosensor to 50 μL of each aliquot were recorded three times. The results, including the added and found choline concentrations, standard deviation, and recovery, are shown in Table 2.

The biosensor demonstrated good recovery, with a recovery rate in the range of 101–107 % and an RSD of 0.4–3.9 % calculated in urine. All

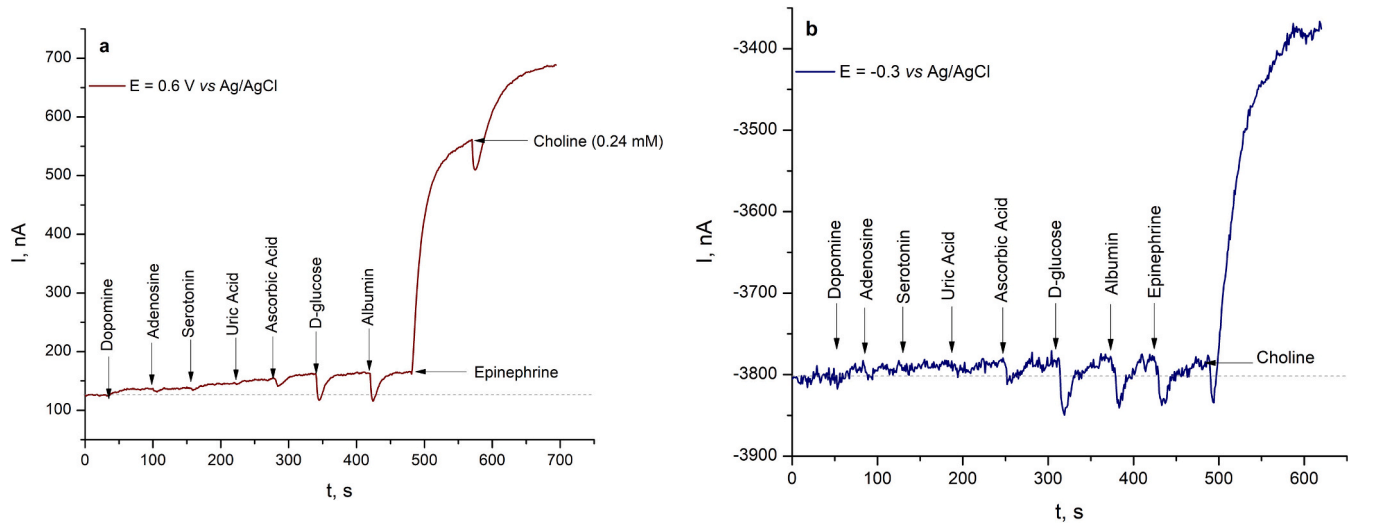

Fig. 5. Influence of interfering compounds on the response currents of dopamine (0.5 μM), adenosine (0.5 μM), serotonin (0.5 μM), uric acid (1 μM), ascorbic acid (2.5 μM), D-glucose (0.05 mM), albumin (70 g/l), epinephrine (24 μM) and choline (0.24 mM) at two different electrode potentials E = +0.6 V *vs* Ag/AgCl (a) and E = −0.3 V *vs* Ag/AgCl (b). PBS (0.01 M; pH 7.2).

Table 2
The analytical performance of the proposed TRGO/ChOx biosensor in urine samples ($n = 3$) was evaluated using the standard addition method. The spike concentration of choline in urine is presented in the first line of the table. E = −0.3 V *vs* Ag/AgCl (b). PBS (0.01 M; pH 7.2).

C(choline added), mM	C(choline found), mM	Recovery, %	RSD, %
0	0.191 ± 0.009	–	–
0.5	0.72 ± 0.01	105	3.34
1	1.302 ± 0.004	107	0.56
1.5	1.701 ± 0.004	103	0.39
2. 5	2.71 ± 0.06	101	3.87

biosensor signals exhibited a slight increase, which could be attributed to the presence of BA and GB. It is evident that the TRGO/ChOx sensor demonstrates favourable sensor accuracy and selectivity at a working potential of −0.3 V. These findings suggest that adaptation of the TRGO/ChOx sensor for the rapid measurement of urine samples is a viable prospect.

4. Conclusions

An amperometric choline biosensor was developed using synthesised thermally reduced graphene oxide (TRGO) as an efficient electrochemical surface and immobilisation matrix for choline oxidase (ChOx). Mechanistic studies revealed that the TRGO/ChOx biosensor can operate *via* two distinct detection pathways depending on the applied working electrode potential: dissolved oxygen (O_2) consumption at −0.3 V and hydrogen peroxide (H_2O_2) oxidation at +0.6 V *vs* Ag/AgCl. This dual behaviour arises from the intrinsic properties of TRGO, including its high surface area and the presence of oxygen-containing functional groups. Due to these features, continuous oxygen reduction reactions (ORR) occur on the TRGO surface at −0.3 V, resulting in a characteristic negative background current. The decrease in ORR is the primary and dominant process, governing the overall operation of the biosensor and its resultant anodic response at −0.3 V. Importantly, this work provides the first detailed description of the operating mechanism of a ChOx-based biosensor functioning at negative electrode potentials.

TRGO/ChOx biosensor exhibited a linear response to choline concentrations of 0.0009–0.24 mM and 0.0008–0.24 mM, with sensitivities of 29 and 38 μA mM^{-1} cm^{-2} at −0.3 V and + 0.6 V *vs* Ag/AgCl, respectively. After 31 days of operation, the TRGO/ChOx biosensor retained 39 % of its initial sensitivity.

The ability to detect choline at a negative operating potential *via* dissolved O_2 consumption greatly enhanced the sensor's analytical characteristics, such as selectivity by minimizing interference from common biological species, including dopamine, adenosine, serotonin, uric acid, ascorbic acid, glucose, albumin, and epinephrine. The excellent TRGO/ChOx biosensor accuracy and selectivity exhibited at a working potential of −0.3 V, highlighting its strong potential for the rapid and reliable detection of choline in urine samples. Considering that this biosensor can also work at a potential of +0.6 V with simple potential switching, such versatility is very useful. These findings lend further support to the feasibility of adapting the TRGO/ChOx biosensor for practical applications in biomedical diagnostics and clinical analysis.

CRediT authorship contribution statement

Ieva Sakinyte-Urbikiene: Writing – review & editing, Writing – original draft, Visualization, Data curation, Conceptualization. **Marius Butkevicius:** Writing – review & editing, Writing – original draft, Validation, Formal analysis, Conceptualization. **Vidute Gureviciene:** Methodology, Data curation. **Liubov Galuzinska:** Resources. **Julija Razumiene:** Writing – review & editing, Supervision, Project administration, Investigation.

Declaration of competing interest

Ieva Sakinyte-Urbikiene, Marius Butkevicius, Vidute Gureviciene, Liubov Galuzinska and Julija Razumiene reports financial support was provided by Research Council of Lithuania. If there are other authors, they declare that they have no known competing financial interests or personal relationships that could have appeared to influence the work reported in this paper.

Acknowledgment

The study was funded by the Research Council of Lithuania (LMTLT) under the the Lithuanian–Ukrainian Cooperation Programme in the Fields of Research and Technologies (Project contract No is S-LU-24-12).

Data availability

Data will be made available on request.

References

[1] M. Song, X. Lin, Z. Peng, S. Xu, L. Jin, X. Zheng, H. Luo, Materials and methods of biosensor interfaces with stability, Front. Mater. 7 (2021) 583739, https://doi.org/10.3389/fmats.2020.583739.

[2] N. Kumari, A. Kumar, R. Prakash, Choline sensing based on enhanced chemiluminescence of luminol-O_2/PDTC@AuNPs system using a smartphone imaging technique, Microchem. J. 186 (2025) 113507, https://doi.org/10.1016/j.microc.2025.113507.

[3] P. Rahimi, Y. Joseph, Enzyme-based biosensors for choline analysis: a review, TrAC, Trends Anal. Chem. 110 (2019) 367–374, https://doi.org/10.1016/j.trac.2018.11.035.

[4] M. Wang, Y. Yang, J. Min, Y. Song, J. Tu, D. Mukasa, C. Ye, C. Xu, N. Heflin, J. S. McCune, T.K. Hsiai, Z. Li, W. Gao, A wearable electrochemical biosensor for the monitoring of metabolites and nutrients, Nat. Biomed. Eng. 6 (2022) 1225–1235, https://doi.org/10.1038/s41551-022-00916-z.

[5] M. Hemdan, M. Hemdan, M.A. Ali, A.S. Doghish, S.S.A. Mageed, I.M. Elaza, M. M. Khalil, M. Mabrouk, D.B. Das, A.S. Amin, Innovations in biosensor technologies for healthcare diagnostics and therapeutic drug monitoring: applications, recent progress, and future research challenges, Sensors 24 (2024) 5143, https://doi.org/10.3390/s24165143.

[6] G. Panfili, P. Manzi, D. Compagnone, L. Scarciglia, G. Palleschi, Rapid assay of choline in foods using microwave hydrolysis and a choline biosensor, J. Agric. Food Chem. 48 (2000) 3403–3407, https://doi.org/10.1021/jf990803%2B.

[7] A. Guerrieri, F. Palmisano, An acetylcholinesterase/choline oxidase-based amperometric biosensors as a liquid chromatography detector for acetylcholine and choline determination in brain tissue homogenates, Anal. Chem. 73 (2001) 2875–2882, https://doi.org/10.1021/ac000852h.

[8] A. Guerrieri, L. Monaci, M. Quinto, F. Palmisano, A disposable amperometric biosensor for rapid screening of anticholinesterase activity in soil extracts, Analyst 127 (2002) 5–7, https://doi.org/10.1039/b109123a.

[9] A. Guerrieri, V. Lattanzio, F. Palmisano, P.G. Zambonin, Electrosynthesized poly (pyrrole)/poly(2-naphthol) bilayer membrane as an effective anti-interference layer for simultaneous determination of acethylcholine and choline by a dual electrode amperometric biosensor, Biosens. Bioelectron. 21 (2006) 1710–1718, https://doi.org/10.1016/j.bios.2005.08.005.

[10] R. Ciriello, S. Lo Magro, A. Guerrieri, Assay of serum cholinesterase activity by an amperometric biosensor based on a co-crosslinked choline oxidase/overoxidized polypyrrole bilayer, Analyst 143 (2018) 920–929, https://doi.org/10.1039/c7an01757j (PMID: 29363680).

[11] A. Guerrieri, R. Ciriello, F. Crispo, G. Bianco, Detection of choline in biological fluids from patients on haemodialysis by an amperometric biosensor based on a novel anti-interference bilayer, Bioelectrochemistry 129 (2019) 135–143, https://doi.org/10.1016/j.bioelechem.2019.05.009.

[12] J. Ahlawat, M. Sharma, C.S. Pundir, An Amperometric acetylcholine biosensor based on co-immobilization of enzyme nanoparticles onto nanocomposite, Biosensors 13 (3) (2023) 386, https://doi.org/10.3390/bios13030386.

[13] F. Arduini, V. Scognamiglio, C. Covaia, A. Amine, D. Moscone, G. Palleschi, A choline oxidase amperometric bioassay for the detection of mustard agents based on screen-printed electrodes modified with prussian blue nanoparticles, Sensors 15 (2015) 4353–4367, https://doi.org/10.3390/s150204353.

[14] M. Özdemir, F. Arslan, H. Arslan, An amperometric biosensor for choline determination prepared from choline oxidase immobilized in polypyrrole-polyvinylsulfonate film, Artif. Cells Blood Substit. Biotechnol. 40 (2012) 280–284, https://doi.org/10.3109/10731199.2011.646411.

[15] R. Baskin, E. Aynaci Koyuncu, H. Arslan, F. Arslan, Development of choline biosensor using toluidine blue O as mediator, Prep. Biochem. Biotechnol. 50 (2020) 240–245, https://doi.org/10.1080/10826068.2019.1687518.

[16] T. Rajarathinam, M. Kwon, D. Thirumalai, S. Kim, S. Lee, J.H. Yoon, H.J. Paik, S. Kim, J. Lee, H.K. Ha, S.C. Chang, Polymer-dispersed reduced graphene oxide nanosheets and Prussian blue modified biosensor for amperometric detection of sarcosine, Anal. Chim. Acta 1175 (2021) 338749, https://doi.org/10.1016/j.aca.2021.338749.

[17] T. Rajarathinam, S. Jayaraman, C.S. Kim, J.H. Yoon, S.C. Chang, Two-dimensional nanozyme nanoarchitectonics customized electrochemical bio diagnostics and lab-on-chip devices for biomarker detection, Adv. Colloid Interf. Sci. 341 (2025) 103474, https://doi.org/10.1016/j.cis.2025.103474.

[18] T. Rajarathinam, D. Thirumalai, S. Jayaraman, S. Yang, A. Ishigami, J. Yoon, H. J. Paik, J. Lee, S.C. Chang, Glutamate oxidase sheets-Prussian blue grafted amperometric biosensor for the real time monitoring of glutamate release from primary cortical neurons, Int. J. Biol. Macromol. 254 (2024) 127903, https://doi.org/10.1016/j.ijbiomac.2023.127903.

[19] T. Rajarathinam, S. Jayaraman, J. Seol, J. Lee, S.C. Chang, Utilizing a disposable sensor with polyaniline-doped multi-walled carbon nanotubes to enable dopamine detection in ex vivo mouse brain tissue homogenates, Biosensors 14 (2024) 262, https://doi.org/10.3390/bios14060262.

[20] A. Weltin, J. Kieninger, G.A. Urban, Microfabricated, amperometric, enzyme-based biosensors for in vivo applications, Anal. Bioanal. Chem. 408 (2016) 4503–4521, https://doi.org/10.1007/s00216-016-9420-4.

[21] S.V. Dzyadevych, V.N. Arkhypova, A.P. Soldatkin, A.V. Elskaya, C. Martelet, N. Jaffrezic-Renault, Amperometric enzyme biosensors: past, present and future, Irbm 29 (2008) 171–180, https://doi.org/10.1016/j.rbmret.2007.11.007.

[22] E. Aynacı, A. Yaşar, F. Arslan, An amperometric biosensor for acetylcholine determination prepared from acetylcholinesterase-choline oxidase immobilized in polypyrrole-polyvinylsulfonate film, Sensors Actuators B Chem. 202 (2014) 1028–1036, https://doi.org/10.1016/j.snb.2014.06.049.

[23] I. Šakinytė, J. Barkauskas, R. Gaidukevič, J. Razumienė, Thermally reduced graphene oxide: the study and use for reagentless amperometric D-fructose biosensors, Talanta 144 (2015) 1096–1103, https://doi.org/10.1016/j.talanta.2015.07.072.

[24] A. Contescu, M. Vass, C. Contescu, K. Putyera, J.A. Schwarz, Acid buffering capacity of basic carbons revealed by their continuous pK distribution, Carbon 36 (1998) 247–258, https://doi.org/10.1016/S0008-6223(97)00168-1.

[25] D. Ratautas, M. Dagys, Nanocatalysts containing direct electron transfer-capable oxidoreductases: recent advances and applications, Catalysts 10 (2019) 9, https://doi.org/10.3390/catal10010009.

[26] B. Liang, L. Fang, G. Yang, Y. Hu, X. Guo, X. Ye, Direct electron transfer glucose biosensor based on glucose oxidase self-assembled on electrochemically reduced carboxyl graphene, Biosens. Bioelectron. 43 (2013) 131–136, https://doi.org/10.1016/j.bios.2012.11.040.

[27] Y. Shao, J. Wang, H. Wu, J. Liu, I.A. Aksay, Y. Lin, Graphene based electrochemical sensors and biosensors: a review, Electroanalysis 22 (2010) 1027–1036, https://doi.org/10.1002/elan.200900571.

[28] L. Jiang, B. van Dijk, L. Wu, C. Maheu, J.P. Hofmann, V. Tudor, M.T.M. Koper, D.G. H. Hetterscheid, G.F. Schneider, Predoped oxygenated defects activate nitrogen-doped graphene for the oxygen reduction reaction, ACS Catal. 12 (2022) 173–182, https://doi.org/10.1021/acscatal.1c03662.

[29] A.V. Kuzmin, B.A. Shainyan, Single Si-doped graphene as a catalyst in oxygen reduction reactions: an in silico study, ACS Omega 5 (2020) 15268–15279, https://doi.org/10.1021/acsomega.0c01303.

[30] S. Lin, J. Tang, K. Zhang, Y. Chen, R. Gao, H. Yin, L.C. Qin, Tuning oxygen-containing functional groups of graphene for supercapacitors with high stability, Nanoscale Adv. 5 (2023) 1163–1171, https://doi.org/10.1039/d2na00506a.

[31] J.D. Wiggins-Camacho, K.J. Stevenson, Mechanistic discussion of the oxygen reduction reaction at nitrogen-doped carbon nanotubes, J. Phys. Chem. C 115 (2011) 20002–20010, https://doi.org/10.1021/jp205336w.

[32] J.M. Goran, J.L. Lyon, K.J. Stevenson, Amperometric detection of l-lactate using nitrogen-doped carbon nanotubes modified with lactate oxidase, Anal. Chem. 83 (2011) 8123–8129, https://doi.org/10.1021/ac2016272.

[33] M. Miyata, Y. Kitazumi, O. Shirai, K. Kataoka, K. Kano, Diffusion-limited biosensing of dissolved oxygen by direct electron transfer-type bioelectrocatalysis of multi-copper oxidases immobilized on porous gold microelectrodes, J. Electroanal. Chem. 860 (2020) 113895, https://doi.org/10.1016/j.jelechem.2020.113895.

[34] S. Liu, B. Wang, B. Liu, S. Dong, Electrochemical behavior of redox species at carbon fibre microdisk array electrode modified with mixed-valent molybdenum (VI, V) oxide, Electrochim. Acta 45 (2000) 1683–1690, https://doi.org/10.1016/S0013-4686(99)00324-2.

[35] R.D. O'Neill, S.C. Chang, J.P. Lowry, C.J. McNeil, Comparisons of platinum, gold, palladium and glassy carbon as electrode materials in the design of biosensors for glutamate, Biosens. Bioelectron. 19 (2004) 1521–1528, https://doi.org/10.1016/j.bios.2003.12.004.

[36] A. Shrivastava, V.B. Gupta, Methods for the determination of limit of detection and limit of quantitation of the analytical methods, Chron. Young. Sci. 2 (2011) 21–25.

[37] G. Gadda, Choline oxidases, Enzymes 47 (2020) 137–166, https://doi.org/10.1016/bs.enz.2020.05.004.

[38] S.K. Bikkarolla, P. Cumpson, P. Joseph, P. Papakonstantinou, Oxygen reduction reaction by electrochemically reduced graphene oxide, Faraday Discuss. 173 (2014) 415–428, https://doi.org/10.1039/C4FD00088A.

[39] S.J. Amirfakhri, D. Binny, J.L. Meunier, D. Berk, Investigation of hydrogen peroxide reduction reaction on graphene and nitrogen doped graphene nanoflakes in neutral solution, J. Power Sources 257 (2014) 356–363, https://doi.org/10.1016/j.jpowsour.2014.01.114.

[40] H.S. Magar, M.E. Ghica, M.N. Abbas, C.M.A. Brett, A novel sensitive amperometric choline biosensor based on multiwalled carbon nanotubes and gold nanoparticles, Talanta 167 (2017) 462–469, https://doi.org/10.1016/j.talanta.2017.02.048.

[41] M. Li, M. Luo, J. An, Y. Liu, Choline electrochemical biosensor based on MWCNT-AuNPs and MWCNT-PANI composite nanomaterials, Microchem. J. 213 (2025) 113609, https://doi.org/10.1016/j.microc.2025.113609.